Structure of Supported Bilayers Composed of Lipopolysaccharides and Bacterial Phospholipids: Raft Formation and Implications for Bacterial Resistance

Jihong Tong and Thomas J. McIntosh
Department of Cell Biology, Duke University Medical Center, Durham, North Carolina

ABSTRACT Lipopolysaccharide (LPS), the major lipid on the surface of Gram-negative bacteria, plays a key role in bacterial resistance to hydrophobic antibiotics and antimicrobial peptides. Using atomic force microscopy (AFM) we characterized supported bilayers composed of LPSs from two bacterial chemotypes with different sensitivities to such antibiotics and peptides. Rd LPS, from more sensitive ''deep rough'' mutants, contains only an inner saccharide core, whereas Ra LPS, from ''rough'' mutants, contains a longer polysaccharide region. A vesicle fusion technique was used to deposit LPS onto either freshly cleaved mica or polyethylenimine-coated mica substrates. The thickness of the supported bilayers measured with contact-mode AFM was 7 nm for Rd LPS and 9 nm for Ra LPS, consistent with previous x-ray diffraction measurements. In water the Ra LPS bilayer surface was more disordered than Rd LPS bilayers, likely due to the greater volume occupied by the longer Ra LPS polysaccharide region. Since deep rough mutants contain bacterial phospholipid (BPL) as well as LPS on their surfaces, we also investigated the organization of Rd LPS/BPL bilayers. Differential scanning calorimetry and x-ray diffraction indicated that incorporation of BPL reduced the phase transition temperature, enthalpy, and average bilayer thickness of Rd LPS. For Rd LPS/BPL mixtures, AFM showed irregularly shaped regions thinner than Rd LPS bilayers by 2 nm (the difference in thickness between Rd LPS and BPL bilayers), whose area increased with increasing BPL concentration. We argue that the increased permeability of deep rough mutants is due to structural modifications caused by BPL to the LPS membrane, in LPS hydrocarbon chain packing and in the formation of BPL-enriched microdomains.

INTRODUCTION

In Gram-negative bacteria an outer membrane, surrounding the cytoplasmic membrane, provides a barrier that plays an important role in the resistance of these bacteria to certain hydrophobic antibiotics and also protects the cells against the lytic effects of antimicrobial peptides. For example, compared to Gram-positive bacteria that lack this outer membrane, Gram-negative bacteria are more resistant to hydrophobic β-lactam antibiotics (Zimmermann and Rosselet, 1977; Nikaido, 1994) and are less susceptible to the peptides magainin and melittin (Macias et al., 1990; Rana et al., 1991; Oren and Shai, 1997; Banemann et al., 1998). The lipid bilayer of the outer membrane is highly asymmetric, as its inner monolayer is composed of phospholipids whereas the outer monolayer is composed mostly of a unique lipid called lipopolysaccharide (LPS) (Nikaido and Vaara, 1985; Raetz, 1993), although phospholipid is also present in the outer monolayers of some bacterial mutants (Kamio and Nikaido, 1976). Therefore, LPS, as the major lipid found on the outer surface of most Gram-negative bacteria, is thought to be a key player in bacterial resistance to hydrophobic antibiotics and antimicrobial peptides (Zimmermann and Rosselet, 1977; Nikaido, 1994; Macias et al., 1990; Rana et al., 1991; Oren and Shai, 1997; Banemann et al., 1998). In addition, LPS is called bacterial endotoxin because it is a nonsecreted toxin that can cause fever and pathology in humans (Raetz, 1993; Rietschel et al., 1994).

LPSs are complex molecules, quite different in composition from membrane phospholipids. As shown in Fig. 1 *A*, LPS consists of a lipid A backbone containing up to seven fatty acid chains with a sizable polysaccharide chain extending from the lipid A (Raetz, 1993; Helander et al., 1996). The polysaccharide portion is further divided into a core oligosaccharide and an O-specific chain, which contains dozens of identical oligosaccharide repeating units. However, bacteria can, either naturally or because of genetic defects, elaborate incomplete LPS lacking the O-specific chain (Helander et al., 1996). Certain mutations that render the bacteria unable to add complete polysaccharide chains to the lipid A backbone cause the bacteria to display a series of characteristics known as ''rough'' or ''deep rough'' phenotypes, depending on the length of the polysaccharide chain. Compared to wild-type bacteria or rough mutants, deep rough mutants have lower resistances to certain hydrophobic antibiotics (Macias et al., 1990; Rana et al., 1991) and antimicrobial peptides such as magainin (Macias et al., 1990; Banemann et al., 1998).

The supramolecular structures of various LPSs have been extensively studied by x-ray diffraction (Burge and Draper, 1967; Kastowsky et al., 1993; Seydel et al., 1993a,b; Kato et al., 1993; Snyder et al., 1999) because of their roles both as a toxin and as a component of the bacterial outer membrane

Submitted November 21, 2003, and accepted for publication February 9, 2004.

Address reprint requests to Thomas J. McIntosh, E-mail: t.mcintosh@cellbio.duke.edu.

0006-3495/04/06/3759/13 $2.00

doi: 10.1529/biophysj.103.037507

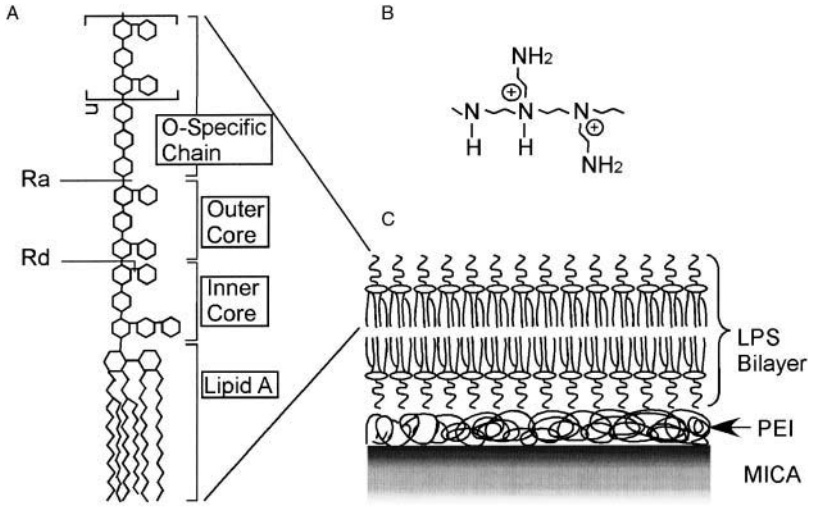

FIGURE 1 Schematic representation of the chemical structures of (*A*) an LPS molecule, (*B*) a PEI monomer, and (*C*) an LPS bilayer on a PEI-coated mica substrate. In (*A*) the lipid acyl chains of the lipid A moiety are represented by jagged lines and the sugar residues of the LPS polysaccharide cores and the O-specific chain are represented by hexagons. Rd LPS contains only the inner saccharide core, whereas the larger Ra LPS contains both the inner and outer saccharide cores.

barrier. That is, the interactions between LPS and cells, antibiotics, and antimicrobial peptides are all thought to depend on LPS aggregation and packing properties (Galanos and Luderitz, 1984; Labischinski et al., 1985; Seydel and Brandenburg, 1990; Brandenburg, 1993; Rietschel et al., 1994; Takayama et al., 1994). Compared to typical phospholipid bilayers, LPS membranes have tighter hydrocarbon chain packing that may play a critical role in its barrier properties (Snyder et al., 1999; Snyder and McIntosh, 2000; Allende and McIntosh, 2003).

Atomic force microscopy (AFM), a technique that allows examination of the morphology of hydrated surfaces with nanometer-level resolution and can provide information complementary to lamellar diffraction data, has been used to analyze the structure of models of eukaryotic cell membrane bilayers, namely phospholipid and phospholipid/cholesterol bilayers deposited on solid substrates such as mica (Shao et al., 1996; Dufrene et al., 1997; Reviakine et al., 1998; Reviakine and Brisson, 2000; Rinia et al., 2000, 2001; Dufrene and Lee, 2000; Janshoff and Steinem, 2001; Yuan et al., 2002). AFM could also be potentially useful in the analysis of models of the outer surface of Gram-negative bacteria and to determine the effects of antimicrobial peptides on LPS organization. To date, analysis by AFM of the outer membrane of Gram-negative bacteria has consisted of images (Amro et al., 2000) and cell adhesion studies (Yao et al., 2002; Velegol and Logan, 2002; Burks et al., 2003; Abu-Lail and Camesano, 2003) of whole cells, and structural investigations of air-dried monolayers (Fukuoka et al., 1994) or crystals (Kato et al., 2000) of an LPS from a deep rough mutant. However, there have been no AFM structural studies of hydrated supported bilayers of LPS, which would provide a more realistic model of the outer membrane than dry monolayers or crystals and should also allow detailed investigations of the structural and interactive properties of specific LPS molecules. As a first and essential step, it is necessary to produce and analyze hydrated supported LPS bilayers. There are potential problems in the preparation of such supported membranes. In particular, since each LPS molecule contains four to six negative charges, it may be difficult to form well-oriented layers on a negatively charged mica sheet.

In this paper we develop techniques to prepare well-oriented, supported LPS membranes. We first prepare LPS bilayers on bare mica and observe their structures under fully and partially hydrated conditions. Next, to minimize electrostatic repulsion between LPS and mica, we precoat mica surfaces with the positively charged polymer polyethylenimine (PEI) (Fig. 1 *B*). Oriented LPS bilayers are formed on the PEI-coated mica surface (Fig. 1 *C*) by incubation with small, unilamellar LPS vesicles. We examine the structure and surface morphology of LPS from both rough (Ra LPS) and deep rough (Rd LPS) mutants by AFM in both fully hydrated and partially dried conditions. The thicknesses of the Ra LPS and Rd LPS bilayers obtained by AFM section analysis are compared to thicknesses previously obtained by x-ray diffraction from multilayers of the same LPSs (Kastowsky et al., 1993; Snyder et al., 1999).

In addition, by a combination of x-ray diffraction, AFM, and differential scanning calorimetry, we analyze the organization and thermal properties of bilayers containing both Rd LPS and bacterial phospholipids (BPL). These studies are of interest for several reasons. First, the antibiotic-susceptible and melittin-sensitive deep rough bacteria contain appreciable amounts of phospholipid in the outer monolayers of their outer membranes (Kamio and Nikaido, 1976). Second, both the permeability of Rd LPS bilayers to hydrophobic antibiotics (Snyder and McIntosh, 2000) and the melittin-induced leakage of LPS bilayers are increased by the addition of BPL to values comparable to those obtained with pure BPL bilayers (Allende and McIntosh, 2003). Moreover, because they contain mostly saturated hydrocarbon chains, the LPS molecule has a very small area per hydrocarbon chain (Snyder et al., 1999), similar to that of

sphingomyelin/cholesterol that forms microdomains in the plane of unsaturated phospholipid bilayers (Rinia et al., 2001; Dietrich et al., 2001). These observations raise the possibility that unsaturated BPL might spontaneously phase-separate from the more tightly packed Rd LPS molecules and form more permeable microdomains in the bilayer. Another possibility is that the addition of BPL could mix with LPS and loosen the LPS hydrocarbon chain packing, thereby increasing the permeability of the bilayer. Therefore, we analyze the structural and thermal properties of Rd LPS/BPL bilayers to determine if BPL forms microdomains in LPS bilayers and/or modifies the LPS hydrocarbon chain packing.

MATERIALS AND METHODS

Materials

Lipopolysaccharides were purchased from Sigma Chemical (St. Louis, MO); the Ra mutant LPS was from *Escherichia coli* EH100 and Rd LPS was from *Salmonella minnesota* R7. Bacterial phospholipid, a polar lipid extract from *E. coli*, was obtained from Avanti Polar Lipids (Alabaster, AL). Polyethylenimine (MW = 2000 D) was purchased from Aldrich Chemical Co. (Milwaukee, WI) as a 50 wt % water solution, and mica disks (10 mm in diameter) were obtained from Ted Pella (Redding, CA). Sodium phosphates (monobasic and dibasic) and Hepes were from Sigma Chemical Co. All reagents were used as received and deionized water (DI) was used to prepare all aqueous solutions.

Vesicle preparation

Multilamellar vesicles (MLVs) of LPS were prepared by adding 1 mg LPS to 1 ml of 25 mM KCl and 5 mM Hepes buffer (pH 7.4), vortexing for at least 1 min, and then incubating the suspension at 60°C for 1 h. To prepare MLVs of LPS/BPL, appropriate amounts of the dry lipids were dissolved in 1.5 ml of petroleum ether/chloroform/phenol (8:5:2) and the solvent was removed by overnight rotary evaporation at 40°C. The lipid films were hydrated by adding 1 ml of 2 and KCl, 5 mM Hepes buffer (pH 7.4), vortexing for 1 min, and then incubating at 60°C for 1 h. Small unilamellar vesicles (SUVs) were prepared by sonicating the MLVs for 10 cycles of 4-min duration (2 min sonication and 2 min standby) at 40 W with a 19-mm flat tip probe sonicator (Misonix, Farmingdale, NY). To sediment any remaining MLVs and titanium particles detached from the probe, the dispersions were centrifuged at 14,000 rpm for 30 min. The supernatants containing the SUVs were stored at 4°C and used to prepare supported LPS and LPS/BPL bilayers.

Modification of mica surface by polyethylenimine

Seventy-five μl of 100 ppm PEI solution in 20 mM Na_2HPO_4/NaH_2PO_4 buffer (pH 6.0) was dropped onto freshly cleaved mica for 30 min at room temperature, rinsed several times with deionized water, and dried with a stream of nitrogen gas. The PEI-coated mica was either scanned by AFM or immediately used for preparation of supported LPS bilayers.

Preparation of supported LPS and LPS/BPL bilayers for AFM analysis

Supported LPS and LPS/BPL bilayers were prepared using the vesicle fusion method (Brian and McConnell, 1984; Shao et al., 1996; Czajkowsky and Shao, 2002). A SUV suspension (75 μl) was applied onto either freshly cleaved or PEI-coated mica. The LPS vesicles were allowed to adsorb and fuse on the surface either at 4°C for overnight or at 60°C for several hours. The LPS/BPL SUVs were applied on PEI-coated mica and heated to 60°C for several hours. Afterwards, the sample was left for several minutes at room temperature and subsequently rinsed with the same buffer used for vesicle preparation. Some samples were subsequently rinsed by DI water. Two types of samples were examined by AFM. Hydrated specimens under buffer or DI water were directly scanned with the AFM, whereas other specimens were dried with a stream of nitrogen before scanning.

Atomic force microscopy

Hydrated samples were scanned by tapping-mode AFM equipped with a fluid cell cantilever holder, whereas the dried samples were scanned by contact-mode AFM. We used a Dimension 3100 AFM with a Nanoscope IIIa controller (Digital Instruments, Santa Barbara, CA) and an oxide-sharpened tip with a spring constant of 0.38 N/m (Digital Instruments). Most of the AFM scans were performed at room temperature. For some LPS/BPL bilayer samples, we used a 100-W lamp to heat the sample to ~40°C (measured with a small thermometer) during the AFM scanning. Images with sizes of 5 μm^2 or 2 μm^2 were obtained at scan rates of 0.5–1.5 Hz. All images shown in this paper were flattened by use of the AFM software. During scanning we set the force as small as possible to obtain a stable and clear image. Tip-induced defects were created by scanning a smaller size of the image at high scan speed (122 Hz) and a high force load for several minutes. By using the Nanoscope software package, we obtained the thickness of the polymer layer and supported LPS bilayer from section analysis, coverage of the LPS bilayers and the coverage ratio of BPL to LPS in LPS/BPL bilayers from bearing analysis, and the root mean square roughness of the surfaces from roughness analysis.

Differential scanning calorimetry

Differential scanning calorimetry (DSC) of Rd LPS and Rd LPS/BPL (1:1) was performed on MLVs (~3 mg/ml) with a VP-DSC microcalorimeter (MicroCal, Northampton, MA). Before beginning a heating cycle the dispersion was incubated at 5°C for 20 min. Samples were cycled at least twice to insure reproducible thermograms. The thermograms were obtained at heating rates of 30°C/h, and the data were analyzed using the MicroCal software.

X-ray diffraction

Wide-angle diffraction patterns were recorded from suspensions of MLVs sealed in capillary tubes and mounted in a point collimation x-ray camera. Low-angle patterns were obtained on oriented multilayers prepared by depositing Rd LPS, BPL, or 1:1 Rd LPS/BPL MLVs on a curved glass surface and drying in a nitrogen atmosphere. The oriented multilayers on the glass substrate were mounted in a temperature-controlled humidity chamber on a single-mirror (line-focused) x-ray camera so that the beam was oriented at a grazing angle relative to the multilayers (McIntosh et al., 1987, 1989; Snyder et al., 1999). Low-angle patterns were recorded at 20°C and 40°C at 86% relative humidity on Kodak DEF x-ray film loaded in flat plate cassette.

RESULTS

LPS vesicle fusion on bare mica

Fig. 2 shows typical AFM images of Rd LPS bilayers on freshly cleaved mica. For the Rd LPS bilayer scanned in water (Fig. 2 *A*), flat areas were observed that were measured

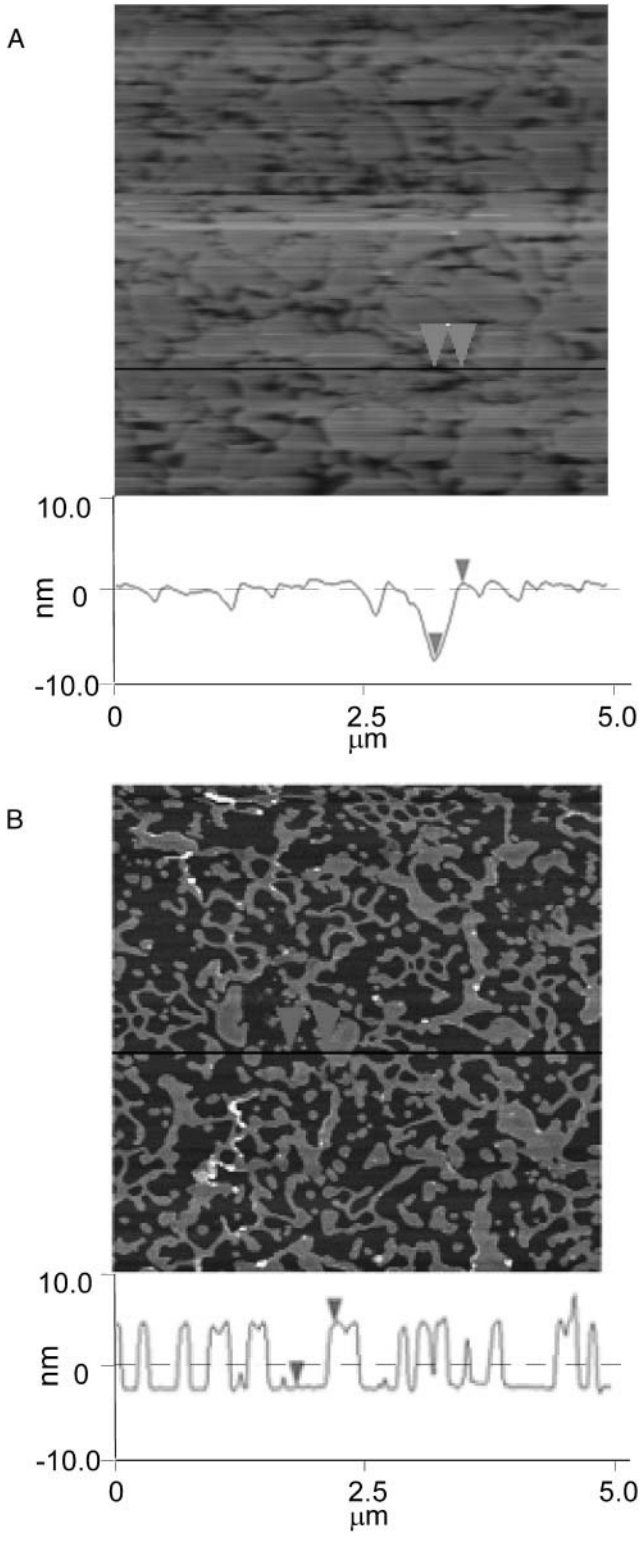

FIGURE 2 AFM images of Rd LPS bilayers on bare mica (*A*) scanned in water (fully hydrated condition) and (*B*) scanned in air (partially hydrated condition). Image size is 5 μm^2 and *z*-scale is 30 nm. In all images lower surfaces are darker. For each image, a section analysis along the horizontal line in the image is shown below the image, with the arrow on the left pointing to the bare mica surface and the arrow on the right pointing to a typical Rd LPS region. From the section analysis the thickness of the Rd LPS is measured to be ~7 nm in each image. The Rd LPS bilayer coverage values are estimated to be 86% in water (*A*) and 36% in air (*B*).

by section analysis to have a thickness of ~7 nm above the mica surface, consistent with the thickness of the Rd LPS bilayer obtained by x-ray diffraction (Kastowsky et al., 1993; Snyder et al., 1999; see Discussion for details). The bilayer coverage was estimated to be ~86%. When the sample was dried by a nitrogen stream and scanned by contact-mode AFM in air (Fig. 2 *B*), flat areas remained, but more defects were observed and there was a smaller surface coverage (36%). From the defects generated after the drying process, we measured the thickness of the Rd LPS bilayer to be 7.0 ± 0.3 nm (mean ± standard deviation of 41 measurements), again the same as x-ray diffraction values for the thickness of Rd LPS bilayers. For both the hydrated (Fig. 2 *A*) and dried (Fig. 2 *B*) specimens, the strong correlation between the thickness of the deposited flat regions and Rd LPS bilayers provides strong evidence that the flat regions are composed of Rd LPS bilayers.

Modification of mica surface by polyethylenimine

To facilitate and improve the preparation of supported bilayers of the anionic LPS, the surface properties of the negatively charged mica were modified with polycationic branched PEI (Sohling and Schouten, 1996; Seitz et al., 1998, 2001; Majewski et al, 1998; Wong et al., 1999a,b; Luo et al., 2001). The preliminary condition required for LPS bilayer preparation is to obtain a flat surface after PEI deposition to insure the subsequent vesicle fusion process of LPS vesicles. Therefore we used AFM to obtain images of the PEI-coated mica surface. As shown in Fig. 3, the PEI-coated mica surface was quite flat, with a roughness of 0.35 nm for the 5-μm^2 scanned area. The polymer layer in the central 1-μm^2 region was removed by the AFM tip at a high force load and a high scan speed. From this artificial defect, we confirmed the formation of the PEI layer and measured its thickness to be ~1.2 nm, which is comparable with the 1.4 nm thickness obtained by Luo et al. (2001).

Structure of supported LPS bilayers on PEI-coated mica

Fig. 4 *A* shows an AFM image of a typical Rd LPS supported bilayer formed on PEI-coated mica scanned by tapping-mode AFM in water and Fig. 4 *B* shows an image of an Rd LPS bilayer on PEI-coated mica scanned by contact-mode AFM in air. A flat Rd LPS bilayer can be seen on the PEI-coated surface in both Fig. 4, *A* and *B*. The Rd LPS bilayer coverage was estimated to be 92% in water and 67% in air, which are better coverages than those obtained on bare mica

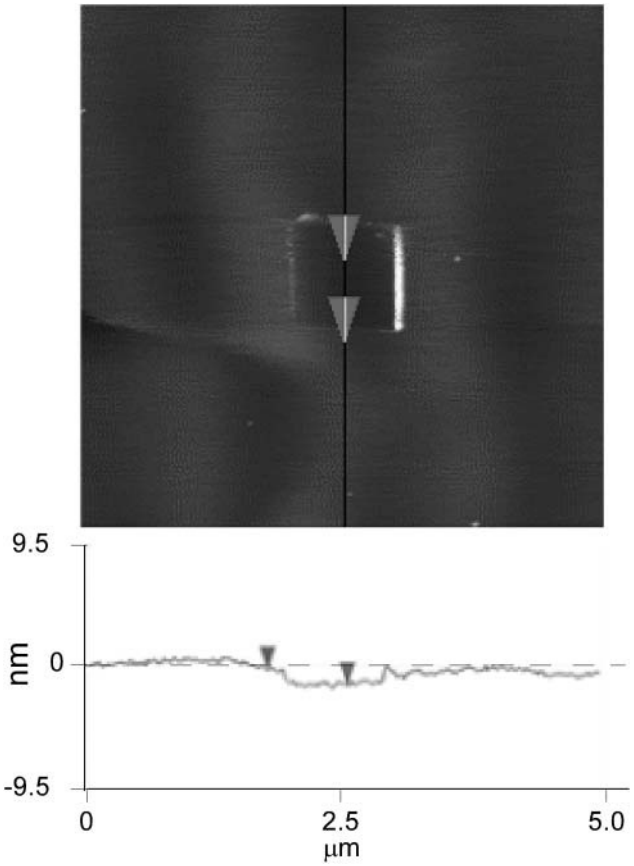

FIGURE 3 AFM image of PEI-coated mica surface, image size is 5 μm^2 and z-scale is 20 nm. A central 1-μm^2 defect was created by the AFM tip at contact mode with a high force load and a high scan speed. A section analysis along the line in the image (shown below the image) gives the thickness of the PEI layer as ~1.2 nm.

with similar incubation conditions. The smaller coverage under partially hydrated conditions indicates that there was reorganization of the bilayer with the dehydration procedure, as was also observed for the Rd LPS bilayer on bare mica. As measured from the lipid surface to the PEI surface (see section analysis of Fig. 4 *B*), the thickness of the lipid layer was 6.9 ± 0.4 nm (50 measurements), equal to that measured for the Rd LPS bilayer on bare mica. Some smaller regions with a lateral size ranging from ~50 to ~200 nm (lightest regions in Fig. 4, *A* and *B*), had a height of ~14 nm above the PEI surface, corresponding to the thickness of two LPS bilayers, indicating the presence of a second bilayer on top of the first bilayer.

We also conducted vesicle fusion of Rd LPS SUVs on PEI-coated mica at 4°C with overnight incubation (data not shown). In that case, when scanned both in water and in air, the Rd LPS bilayers had the same thickness as, but poorer surface coverage than, those prepared at 60°C with 3 h incubation. Fewer double-bilayer elevations, as seen in Fig. 4 *A*, were observed on the samples prepared at 4°C.

AFM images of Ra LPS supported bilayers scanned by tapping-mode AFM in water and contact-mode AFM in air are shown in Figs. 5, *A* and *B*, respectively. The coverage of the Ra LPS bilayer after drying was 46% (Fig. 5 *B*), which was smaller than that of the Rd LPS bilayer on PEI-coated mica (Fig. 4 *B*), and fewer double-bilayer structures were observed compared with that of Rd LPS bilayers. Section analyses of Fig. 5 *B* gave the height of the Ra LPS surface above the PEI layer as 8.8 ± 0.6 nm (50 measurements), which is similar to the thickness of the LPS bilayers as obtained from x-ray diffraction (Kastowsky et al., 1993; Snyder et al., 1999). When dried, both Ra and Rd bilayers were quite smooth. However, compared to fully hydrated Rd LPS bilayer (Fig. 4 *A*), the surface morphology of Ra LPS bilayer in water (Fig. 5 *A*) was much more uneven.

Differential scanning calorimetry of Rd LPS and Rd LPS/BPL

Differential scanning calorimetry thermograms of Rd LPS and equimolar Rd LPS/BPL MLVs are shown in Fig. 6. Rd LPS bilayers gave a thermal phase transition at ~29°C with an enthalpy of 8.4 kcal/mol. This result is in good agreement with previous work showing that LPSs of rough mutants from various organisms had phase transitions between 20 and 37°C (Brandenburg and Seydel, 1984; Rodriguez-Torres et al., 1993) with enthalpies ranging from 5.8 to 12.6 kcal/mol (Rodriguez-Torres et al., 1993). In contrast, we found that 1:1 Rd LPS/BPL bilayers displayed a broader transition at ~24°C with an enthalpy of only 1.1 kcal/mol (Fig. 6).

X-ray diffraction of LPS/BPL bilayers

X-ray patterns from unoriented MLV suspensions of Rd LPS, BPL, and 1:1 Rd LPS/BPL at 20°C gave single wide-angle diffraction bands whose spacing and width depended on the specimen. Rd LPS gave a single sharp reflection at 0.42 nm, whereas BPL or 1:1 Rd LPS/BPL gave a very broad wide-angle band centered at 0.45 nm.

Low-angle x-ray diffraction patterns for oriented multilayers of Rd LPS, BPL, and Rd LPS/BPL were recorded at temperatures both below (20°C) and above (40°C) the phase transition temperature of Rd LPS (BPL is in a liquid-crystalline phase at both temperatures). The lamellar repeat periods recorded at 86% relative humidity are shown in Table 1. At this relative humidity the interbilayer fluid spaces are very narrow, so that the lamellar repeat periods provide a good estimate for the total bilayer thickness (McIntosh et al., 1987, 1989; Snyder et al., 1999). For all experiments shown in Table 1, reflections corresponding to orders of a single lamellar repeat period were recorded. Five or six orders of diffraction were recorded for Rd LPS or BPL, but only one or two relatively broad orders of diffraction were recorded for Rd LPS/BPS mixtures. For both temperatures, the repeat periods for Rd LPS were ~2 nm larger than those of BPL, and the repeat periods of the Rd LPS/BPL mixtures were between the values for Rd LPS and BPL.

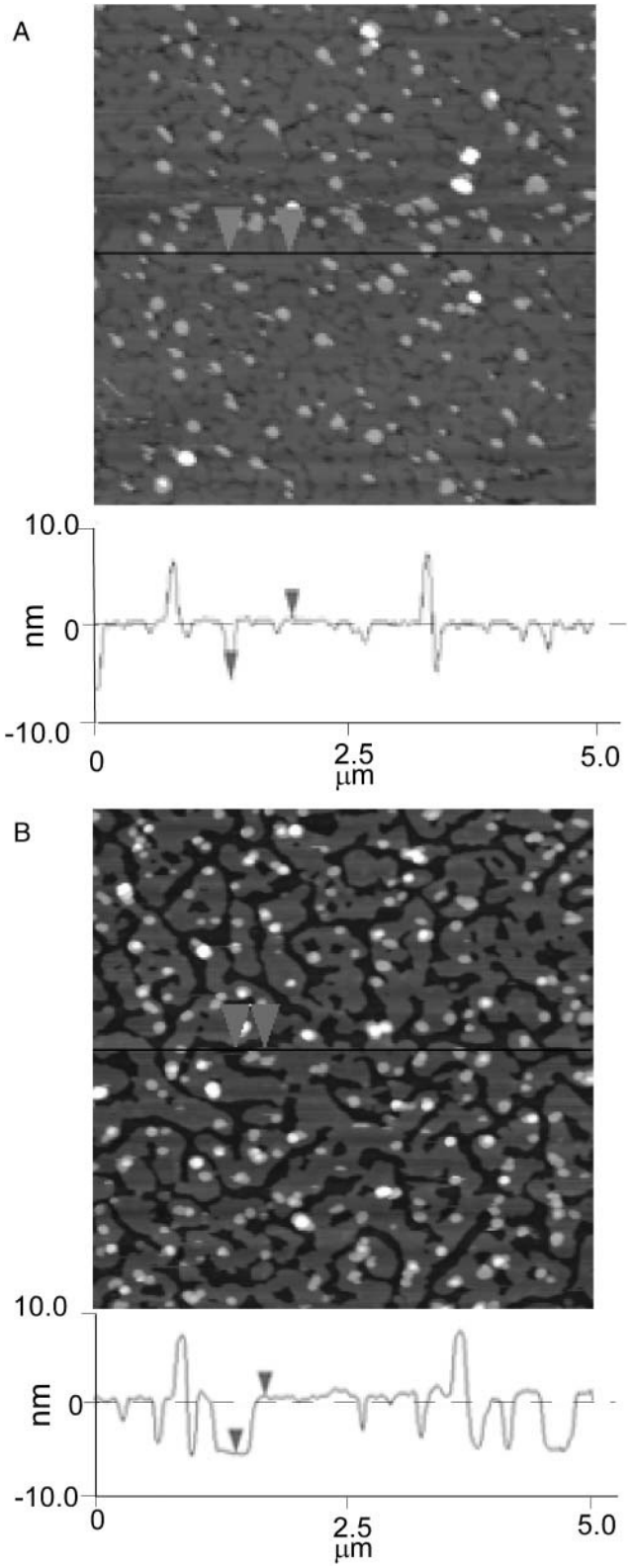

FIGURE 4 AFM images of Rd LPS bilayers formed on PEI-coated mica (*A*) scanned in water and (B) scanned in air. Image size, 5 μm^2; *z*-scale, 30 nm. For each image, a section analysis along the horizontal line in the image is shown below the image, with the arrow on the left pointing to the PEI-coated mica surface and the arrow on the right pointing to a typical LPS bilayer region. From the section analysis the thickness of the bilayer is measured to be ~7 nm in each image. The Rd LPS bilayer coverage values on PEI-coated mica are estimated to be 92% in water and 67% in air. The highest peaks in the section analysis of Rd LPS have a height of 14 nm and probably correspond to a double bilayer region.

Surface morphology of Rd LPS/BPL bilayers on PEI-coated mica

AFM scans of hydrated Rd LPS/BPL supported bilayers on PEI-coated mica were obtained at 20°C (Fig. 7) and at 40°C (Fig. 8). At 20°C, both 1:1 Rd LPS/BPL (Fig. 7 *A*) and 2:1 Rd LPS/BPL (Fig. 7 *B*) gave scans primarily composed of irregularly shaped areas of two different heights. As shown in the section analyses under each scan, the difference in height between the two levels was ~2 nm, which is approximately equal to the difference in repeat period of Rd LPS and BPL (Table 1). Thus, as a working hypothesis, we assume that the higher and lower regions correspond to microdomains enriched in LPS and BPL, respectively. The average lateral dimensions of the low (BPL-enriched) domains were quite small (~20–150 nm). The images and section analyses indicated that there was a higher percentage of the BPL-enriched surface for 1:1 Rd LPS/BPL than for 2:1 Rd LPS/BPL. We used the AFM to determine quantitatively the relative fraction of BPL-enriched domain for several Rd LPS and BPL mixtures, and compared those values to values predicted assuming separate LPS and BPL phases. In this calculation we assumed that Rd LPS contained six acyl chains, with each chain having an area of 0.26 nm^2 (Snyder et al., 1999), and the area for BPL was calculated assuming that the average area per acyl chain was 0.30 nm^2 and that the BPL from Avanti Polar lipids contained 23% phosphatidylethanolamine and 67% phosphatidylglycerol (both with two acyl chains per molecule) and 10% cardiolipin (four acyl chains per molecule). As shown in Fig. 9, there was a linear correlation between the measured and expected percentage of the low (BPL-enriched) regions for 2:1, 1:1, 1:2, and 1:3 Rd LPS/BPL bilayers.

At 40°C, for both 1:1 Rd LPS/BPL (Fig. 8 *A*) and 2:1 Rd LPS/BPL (Fig. 8 *B*), regions at different levels were observed with the difference in height of ~2 nm. However, at 40°C (Fig. 8) the boundaries of the domains were less distinct than they were at 20°C (Fig. 7), so that the quite small (lateral dimensions of 20–100 nm) BPL-enriched domains were more difficult to see. At 40°C there was also a correlation between the measured and expected LPS domain area with changing LPS/BPL composition (Fig. 9).

DISCUSSION

Supported phospholipid bilayers have been extensively studied by AFM, which has been proven to be a useful technique for providing high-resolution structural infor-

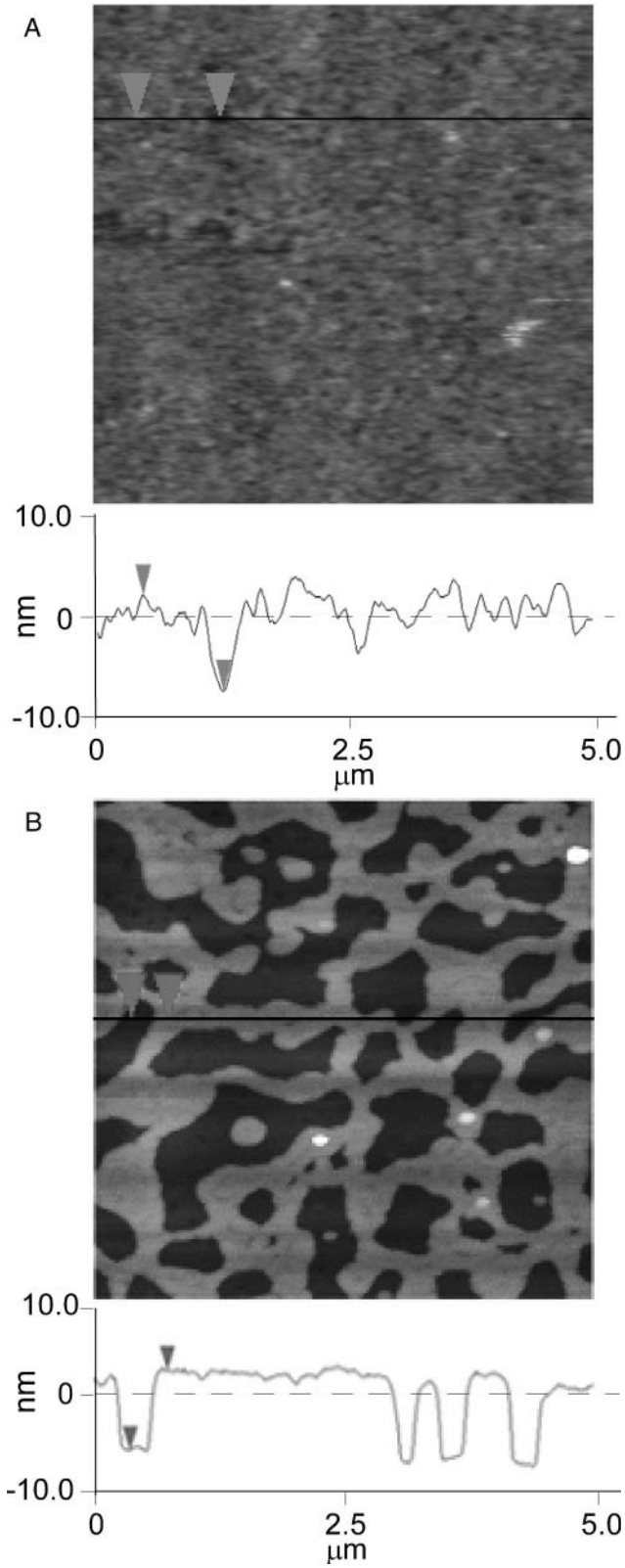

FIGURE 5 AFM images of Ra LPS bilayers formed on PEI-coated mica by 4 h SUV deposition at 60°C: (*A*) scanned in water and (*B*) scanned in air. Image size: 5 × 5 μm, *z*-scale: 30 nm. For each image, a section analysis along the horizontal line in the image is shown below the image, with the lower arrow pointing to the PEI-coated mica surface and the upper arrow pointing to a typical LPS bilayer region. From the section analysis the thickness of the bilayer is measured to be ~9 nm in each image.

mation on bilayer surface morphology (Shao et al., 1996; Dufrene et al., 1997; Reviakine et al., 1998; Reviakine and Brisson, 2000; Rinia et al., 2000, 2001; Dufrene and Lee, 2000; Janshoff and Steinem, 2001; Yuan et al., 2002) and bilayer interactions with membrane proteins (Shao et al., 1996; Reviakine et al., 1998; Rinia et al., 2000; Yuan et al., 2002). Due to the importance of LPS in the surface properties of Gram-negative bacteria, in this study we have prepared supported bilayers of LPS as models for the bacterial outer membrane and have characterized these bilayers by AFM.

To form LPS bilayers, we used the vesicle fusion method (Shao et al., 1996; Brian and McConnell, 1984; Czajkowsky and Shao, 2002), which has been an effective preparation technique for forming supported bilayers with one or more phospholipid components (Dufrene and Lee, 2000; Rinia et al., 2000, 2001; Zhang et al., 2000, 2002). A challenge with this fusion method (Shao et al., 1996; Brian and McConnell, 1984; Czajkowsky and Shao, 2002) is that it is difficult to prepare supported bilayers containing high contents of negatively charged lipids (such as LPS) on negatively charged substrates such as mica. Phospholipid bilayers have previously been formed on polymer cushions absorbed to mica or other substrates using polyelectrolytes such as PEI or other polymers as the cushion (Sohling and Schouten, 1996; Majewski et al, 1998; Seitz et al., 1998, 2000, 2001; Wong et al., 1999a,b; Zhang et al., 2000, 2002; Wagner and Tamm, 2000; Luo et al., 2001). Since PEI is highly positively charged at low pH (Claesson et al., 1997; Pfau et al., 1999), we expected that the deposition of this branched polyelectrolyte on a mica surface would improve the LPS vesicle fusion process due to electrostatic interaction and allow uniform supported LPS bilayers. In addition, such polymer-supported bilayers are likely more suitable fluid model systems to study protein lipid interactions than are bilayers attached directly to solid surfaces (Wagner and Tamm, 2000; Seitz et al., 2001). The data in this paper show that precoating of the mica with PEI dramatically improved the LPS surface coverage without changing the thickness of the LPS bilayer.

Rd LPS bilayers formed on bare mica

We found that the Rd LPS bilayer on mica was fairly smooth, with 86% coverage (Fig. 2 *A*) in water. Thus, although there should be electrostatic repulsion between the negatively charged LPS and the bare mica surface, there was still relatively good coverage. This could be in part due to screening of electrostatic repulsion by the presence of cations in a thin layer of buffer solution between the mica and the Rd

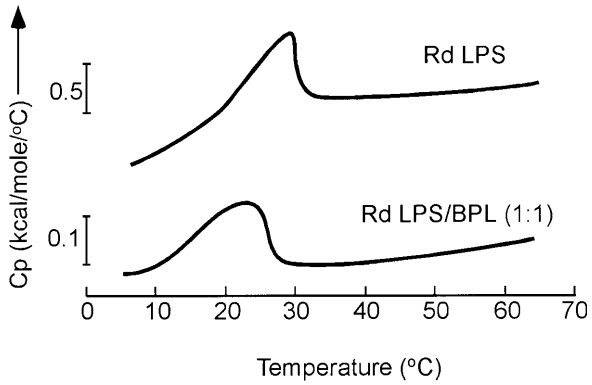

FIGURE 6 DSC thermograms of Rd LPS (3 mg/ml) and equimolar Rd LPS/BPL (4 mg/ml) MLVs. Note that the two thermograms are shown on different vertical scales. The arrow points in the direction of an endothermic transition.

LPS bilayer. Such thin aqueous layers are thought to exist between mica and a bilayer (Shao et al., 1996; Rinia et al., 2001). When the bilayer was dried by nitrogen stream the coverage was only 36% (Fig. 2 *B*). This partial drying could remove some of the water layer between mica and the bilayer, increasing the electrostatic repulsion between the substrate and lipid. Thus, it appears that the water content was a key factor for maintenance of the bilayer in a quasistable state on bare mica.

Polyethylenimine coating of the mica surface

Our PEI coating was 1.2 nm thick, which can be compared to previous values for PEI thickness of 1.4 nm (Luo et al., 2001), 0.6 nm (Sohling and Schouten, 1996), 0.6–1.5 nm (Pfau et al., 1999), and 10 nm or more (Majewski et al., 1998; Wong et al., 1999a). The exact thickness of the PEI layer apparently depends on the molecular weight of the PEI and the deposition method. Our PEI surface was a little rougher (0.35 nm over a 5 μm^2 area) than that of our bare mica surface (0.19 nm over a 5 μm^2 area). By comparison, Senden and Ducker (1992) reported the roughness of plasma-treated mica to be ~0.13 nm over a 670 nm^2 area, whereas Zhang et al. (2002) found the roughness of an Au layer formed on mica to be 1.02 ± 0.08 nm over a 2 μm^2 area. Thus, compared to such an Au layer on mica, the PEI-coated mica layers provided smoother surfaces for the formation of supported bilayers.

TABLE 1 Lamellar repeat periods for Rd LPS and BPL multilayers

Temperature (°C)	Rd LPS	BPL	1:1 Rd LPS/BPL	1:2 Rd LPS/BPL	1:3 Rd LPS/BPL
20°C	6.8 nm	4.9 nm	–	6.2 nm	5.9 nm
40°C	6.4 nm	4.5 nm	6.1 nm	6.1 nm	5.8 nm

LPS bilayers on PEI-coated mica

Compared with the Rd LPS bilayers formed on bare mica scanned in water or in air (Fig. 2), there was improved LPS coverage on PEI-coated mica (Fig. 4). Moreover, the Rd LPS bilayer on the PEI-coated mica was more stable against drying (Figs. 2 *B* and 4 *B*), as the retained coverage in air increased from 36% on bare mica to 67% on PEI-coated mica. Thus, PEI improved bilayer formation and maintenance during partial dehydration. With the PEI-coated mica, the vesicle fusion method reproducibly gave stable and smooth Rd LPS bilayers.

Supported bilayers on PEI-coated mica could also be formed from Ra LPS, which has a longer saccharide core region and a higher number of charges per molecule (Helander et al., 1996) than Rd LPS (Fig. 1 *B*). As can be seen from Figs. 4 *A* and 5 *A*, when the samples were scanned in water the surface of the Ra LPS bilayer sample was significantly more uneven and disordered than the Rd LPS surface. We argue that this increased roughness was due to the longer saccharide chain of Ra LPS taking up more water, occupying more volume, and being more disordered than the shorter saccharide core of Rd LPS.

Comparison with x-ray diffraction data

Kastowsky et al. (1993) recorded diffraction patterns from partially hydrated multilayers and Snyder et al. (1999) carried out x-ray diffraction/osmotic stress experiments on several rough and deep rough mutant LPSs, including the same Ra LPS and Rd LPS analyzed in Figs. 2, 4, and 5. For both our AFM scans and these x-ray diffraction analyses (Kastowsky et al., 1993; Snyder et al., 1999), the LPS bilayers are in the gel phase at room temperature. In excess buffer, both Ra and Rd LPS gave broad low-angle diffraction bands indicating that there is a large, irregular fluid space between adjacent bilayers due to the electrostatic repulsion between the bilayers (Snyder et al., 1999). To stack the bilayers in regular arrays so that x-ray diffraction could be recorded, Snyder et al. (1999) systematically removed the interbilayer water by applying osmotic pressure. Analysis of these osmotic stress/x-ray diffraction data showed that the total bilayer thickness was ~9 nm and 7 nm for Ra LPS and Rd LPS, respectively, in excellent agreement with the thicknesses measured here by AFM. Thus, the deposition of SUVs on the PEI-coated mica surfaces preserved the structure of the LPS bilayers. Since electron density profiles indicate that the thickness of the lipid A portion of the Ra and Rd LPS is the same, the difference in bilayer thickness must be due to the difference in length of the polysaccharide regions of the molecules (Snyder et al., 1999). Moreover, comparisons of the bilayer thicknesses with thicknesses calculated from molecular packing models (Snyder et al., 1999) indicate that the Ra and Rd LPS molecules in supported bilayers are oriented approximately perpendicular

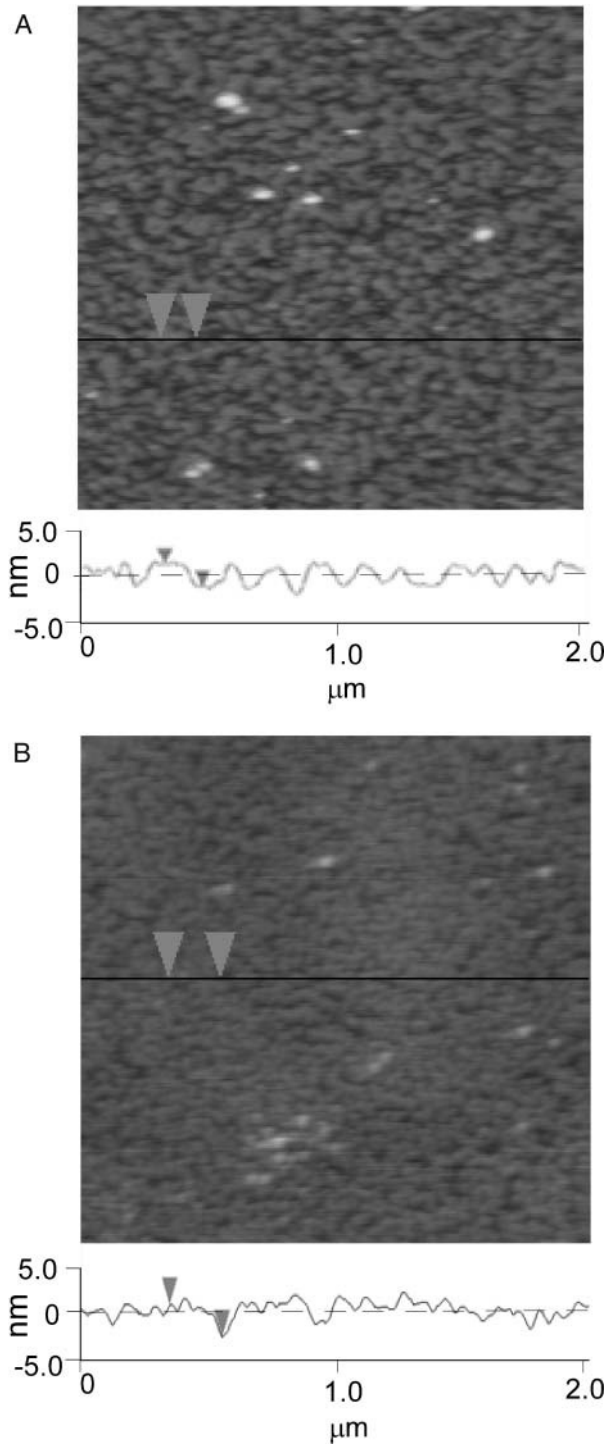

FIGURE 7 AFM images of (*A*) 1:1 Rd LPS/BPL and (*B*) 2:1 Rd LPS/BPL formed on PEI-coated mica scanned in water at 20°C. Image size, 2 μm^2; *z*-scale, 20 nm. For each image, regions of two different thicknesses are observed. A section analysis along the horizontal line in the image is shown below the image, indicating that the difference in height of the two regions is ~2 nm.

to the bilayer surface, as they are in multilayers (Kastowsky et al., 1993; Snyder et al., 1999).

Comparison with AFM studies of supported phospholipid bilayers

The structures of the hydrated supported LPS bilayers (Figs. 4 *A* and 5 *A*) differ in two important ways from that of typical supported phospholipid bilayers. First, the thicknesses of 9 nm and 7 nm for Ra LPS and Rd LPS bilayers, respectively, are greater than the 4–6 nm thicknesses typically observed from supported phospholipid bilayers (Janshoff and Steinem, 2001; Rinia et al., 2000, 2001). This difference must be largely due to the presence of the polysaccharide chains of LPSs. In addition, the disordered, uneven surface morphology of hydrated Ra LPS bilayer (Fig. 5 *A*) contrasts with the flat surface morphology typically obtained for single-component phospholipid bilayers. As noted above, we argue that the uneven surface of Ra LPS bilayer is caused by the relatively long polysaccharide chain of Ra LPS.

Structure and thermal properties of Rd LPS/BPL bilayers

The incorporation of BPL decreased the phase transition temperature and the enthalpy of Rd LPS bilayers. The wide-angle x-ray diffraction patterns indicated that the addition of BPL modified the hydrocarbon chain packing of Rd LPS below its phase transition temperature, converting a sharp reflection, indicative of ordered hydrocarbon chains, to a broader reflection, characteristic of more disorder in the hydrocarbon chain packing (Tardieu et al., 1973). Even though there was a quite low enthalpy phase transition for 1:1 Rd LPS/BPL (Fig. 6), we were unable to detect a sharp wide-angle reflection for 1:1 Rd LPS/BPL.

The low-angle x-ray diffraction data indicated that the incorporation of BPL reduced the lamellar repeat period of Rd LPS (Table 1), so that the repeat period was between that of Rd LPS and BPL. Moreover, for all Rd LPS/BPL ratios analyzed, a single repeat period was observed. These results indicate that there was molecular mixing of Rd LPS and BPL, with no three-dimensional phase separation. That is, the changes in thermal properties and repeat period indicate that Rd LPS and BPL occupied the same bilayers and that BPL modified the organization of the Rd LPS bilayer.

Microdomains or rafts ranging in later dimensions from 100 nm to 20 μm have been detected by AFM in specific mixtures of dioleoylphosphatidylcholine (DOPC), sphingomyelin (SM), and cholesterol (Rinia et al. 2001). SM/cholesterol-enriched domains in a DOPC matrix can be visualized by AFM because the SM/cholesterol bilayer is ~1 nm thicker than a DOPC bilayer (Rinia et al. 2001; Gandhavadi et al., 2002). With the DOPC/SM/cholesterol preparation large domains (5–20 μm) have also been

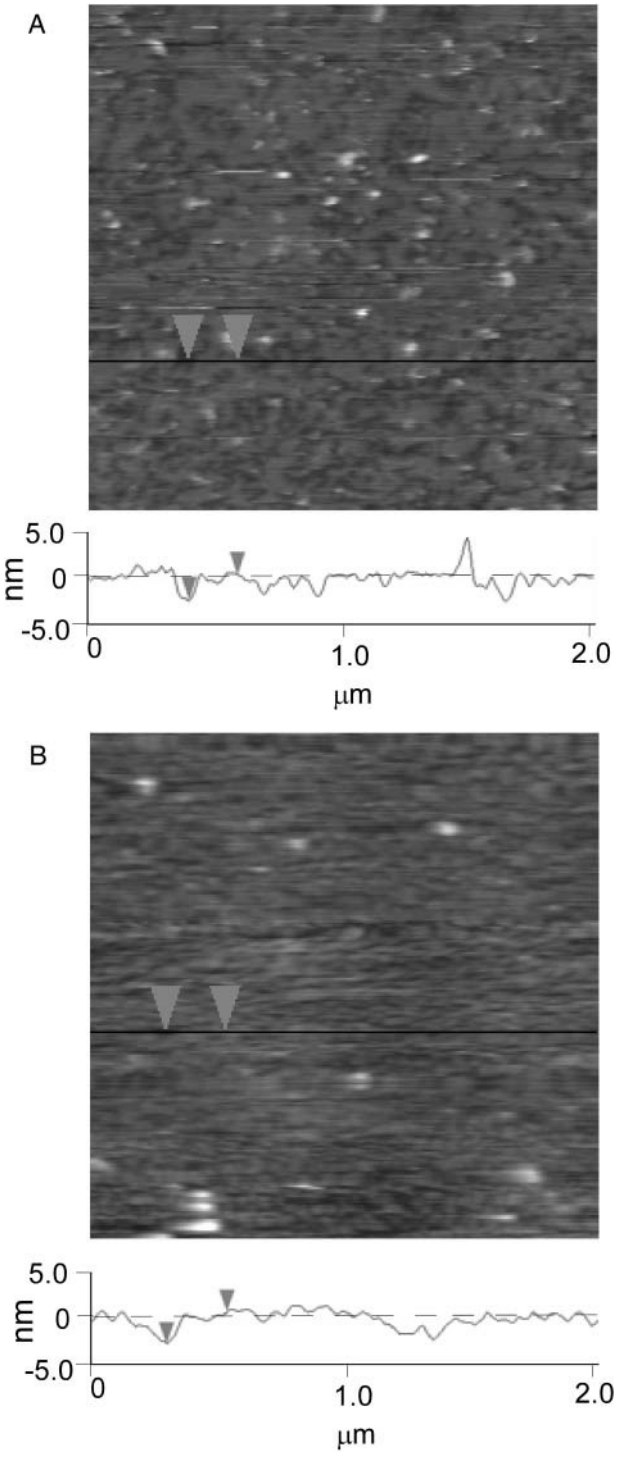

FIGURE 8 AFM images of (*A*) 1:1 Rd LPS/BPL and (*B*) 2:1 Rd LPS/BPL bilayers formed on PEI-coated mica, scanned in water at 40°C. Image size, 2 μm^2; *z*-scale, 20 nm. For each image, a section analysis along the horizontal line in the image is shown below the image.

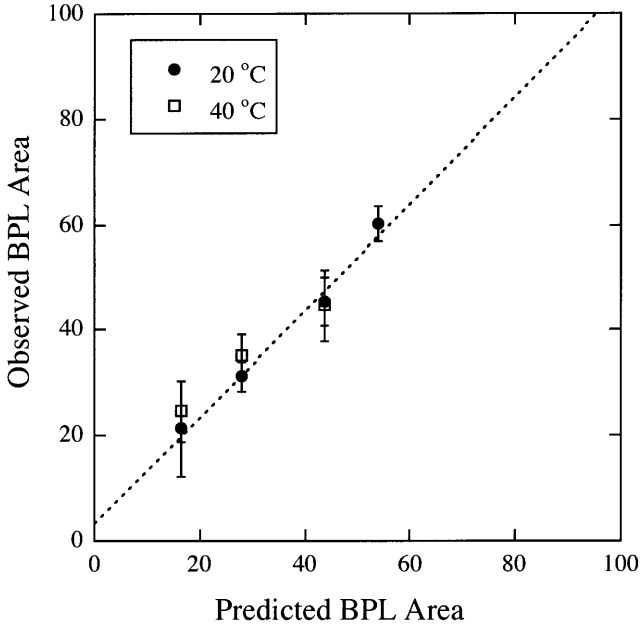

FIGURE 9 Relationship between the predicted and observed BPL area in Rd LPS/BPL supported bilayers at 20°C and 40°C. Error bars represent standard deviations for three to five different AFM scans, and the dotted line is a least-squares fit to the 20°C values ($R^2 = 0.986$).

observed by fluorescence microscopy in giant unilamellar lipid vesicles (Dietrich et al., 2001; Veatch and Keller, 2003) or unsupported planar bilayers (Samsonov et al., 2001).

Because the thickness of Rd LPS and BPL differ by ~2 nm, if microdomains formed in Rd LPS/BPL mixtures, they should be visible by AFM. At temperatures below the thermal phase transition of Rd LPS (Fig. 7), very small (20–150 nm) domains of the correct relative thickness could be detected. At temperatures above the phase transition of Rd LPS the putative domains were even smaller, less distinct, and more difficult to detect. Thus, our AFM images do not show the large (micrometer-sized) rafts visible in DOPC/SM/cholesterol preparations. The observed differences in domain size between DOPC/SM/cholesterol (Rinia et al., 2001) and Rd LPS/BPL (Fig. 8) could be due to differences in line tensions between the two systems. Line tensions have been shown to be important in determining the shape of bilayer domains (Baumgart et al., 2003). If the line tensions for LPS domains in BPL were less than those for SM/cholesterol domains in DOPC, then the LPS domains would be expected to be smaller, as larger domains minimize edge energy, but at an entropic cost. The LPS polysaccharide head groups could modify line tensions, as the inclusion of glycolipids has been shown to modify the hydrophilic pore edge line tension of lipid membranes (Melikyan et al., 1990).

Thus, the DSC and x-ray diffraction experiments showed that Rd LPS and BPL mix in the plane of the bilayer, modifying the thermal properties, hydrocarbon chain

packing, and average bilayer width. AFM experiments showed that, although large rafts or microdomains were not found in mixtures of Rd LPS and BPL, relatively small BPL-enriched microdomains were present.

Finally, we relate our structural observations to previous observations on interactions of hydrophobic antibiotics (Snyder and McIntosh, 2000) and melittin (Allende and McIntosh, 2003) with large unilamellar vesicles (LUVs) composed of LPS and BPL. Those experiments indicate that tight hydrocarbon chain packing decreases the permeability of LUVs to hydrophobic antibiotics (Snyder and McIntosh, 2000) and also decreases melittin-induced vesicle leakage (Allende and McIntosh, 2003). We argue that either the observed BPL-induced changes in LPS hydrocarbon chain packing or the formation of BPL-enriched domains would provide looser hydrocarbon chain packing environments that could increase antibiotic permeability across the bilayer and increase bilayer susceptibility to antimicrobial peptides. In the above comparison of published permeability/leakage data (Snyder and McIntosh, 2000; Allende and McIntosh, 2003) and our AFM measurements, a complicating factor is the currently unknown relationship between the organization of LPS/BPL in LUV bilayers and in supported bilayers formed by SUV fusion. Two observations indicate the validity of the supported bilayers as accurate models for unsupported bilayers. First, the difference in thickness of the domains observed by AFM is exactly the thickness difference between BPL and Rd LPS bilayers as measured by x-ray diffraction from both supported and unsupported multibilayers. Second, the coverages of the observed bilayer domains vary predictably with bilayer composition (Fig. 9).

We thank Dr. Homme Hellinga of the Department of Biochemistry at Duke University Medical Center for use of the AFM facility, Dr. Jeff Smith of that department for advice on the AFM experiments, and Dr. Sid Simon of the Department of Neurobiology at Duke University Medical Center for help with the DSC experiments.

This work was supported by grants GM27278 and GM58432 from the National Institutes of Health.

REFERENCES

Abu-Lail, N. I., and T. A. Camesano. 2003. Role of lipopolysaccharides in the adhesion, retention, and transport of *Escherichia coli* JM109. *Environ. Sci. Technol.* 37:2173–2183.

Allende, D., and T. J. McIntosh. 2003. Lipopolysaccharides in bacterial membranes act like cholesterol in eukaryotic membranes in providing protection against melittin-induced bilayer lysis. *Biochemistry.* 42:1101–1108.

Amro, N. A., L. P. Kotra, K. Wadu-Mesthrige, A. Bulychev, S. Mobashery, and G. Liu. 2000. High-resolution atomic force microscopy studies of the *Escherichia coli* outer membrane: structural basis for permeability. *Langmuir.* 16:2789–2796.

Banemann, A., H. Deppisch, and R. Gross. 1998. The lipopolysaccharide of *Bordetella bronchiseptica* acts as a protective shield against antimicrobial peptides. *Infect. Immunol.* 66:5607–5612.

Baumgart, T., S. T. Hess, and W. W. Webb. 2003. Imaging coexisting fluid domains in biomembrane models coupling curvature and line tension. *Nature.* 425:821–824.

Brandenburg, K. 1993. Fourier transform infrared spectroscopy characterization of the lamellar and nonlamellar structures of free lipid A and Re lipopolysaccharides from *Salmonella minnesota* and *Escherichia coli*. *Biophys. J.* 64:1215–1231.

Brandenburg, K., and U. Seydel. 1984. Physical aspects of structure and function of membranes made from lipopolysaccharides and free lipid A. *Biochim. Biophys. Acta.* 775:225–238.

Brian, A. A., and H. M. McConnell. 1984. Allogeneic stimulation of cytotoxic T cells by supported planar membranes. *Proc. Natl. Acad. Sci. USA.* 81:6159–6163.

Burge, R. E., and J. C. Draper. 1967. The structure of the cell wall of the Gram-negative bacterium *Proteus vulgaris*. III. A lipopolysaccharide ''unit membrane. *J. Mol. Biol.* 28:205–210.

Burks, G. A., S. B. Velegol, E. Paramonova, B. E. Lindenmuth, J. D. Feick, and B. E. Logan. 2003. Macroscopic and nanoscale measurements of the adhesion of bacteria with varying outer layer surface composition. *Langmuir.* 19:2366–2371.

Claesson, P. M., O. E. H. Paulson, E. Blomberg, and N. L. Burns. 1997. Surface properties of poly(ethyleneimine)-coated mica surfaces—salt and pH effects. *Coll. Surf. A.* 123:341–353.

Czajkowsky, D. M., and Z. Shao. 2002. Supported lipid bilayers as effective substrates for atomic force microscopy. *In* Methods in Cell Biology, Vol. 68: Atomic Force Microscopy in Cell Biology. B. P. Jena and J. K. H. Horber, editors. Academic Press, New York. 231–241.

Dietrich, C., L. A. Bagatolli, Z. N. Volovyk, N. L. Thompson, M. Levi, K. Jacobson, and E. Gratton. 2001. Lipid rafts reconstituted in model membranes. *Biophys. J.* 80:1417–1428.

Dufrene, Y. F., W. R. Barger, J.-B. D. Green, and G. U. Lee. 1997. Nanometer-scale surface properties of mixed phospholipid monolayers and bilayers. *Langmuir.* 13:4779–4784.

Dufrene, Y. F., and G. U. Lee. 2000. Advances in the characterization of supported lipid films with the atomic force microscope. *Biochim. Biophys. Acta.* 1509:14–41.

Fukuoka, S., M. Matsumoto, R. Azumi, and I. Karube. 1994. Thin film formation by rough form lipopolysaccharide and interaction with cationic antibiotic polymyxin B. *Microbiosystems.* 78:169–176.

Galanos, C., and O. Luderitz. 1984. Lipopolysaccharide: properties of an amphipathic molecule. *In* Handbook of Endotoxin, Vol. 1. Chemistry of Endotoxin. E. T. Rietschel, editor, Elsevier, Amsterdam, The Netherlands. 46–58.

Gandhavadi, M., D. Allende, A. Vidal, S. A. Simon, and T. J. McIntosh. 2002. Structure, composition, and peptide binding properties of detergent soluble bilayers and detergent resistant rafts. *Biophys. J.* 82:1469–1482.

Helander, I. M., P. H. Makela, O. Westphal, and E. T. Rietschel. 1996. Lipopolysaccharides. *In* Encyclopedia of Molecular Biology and Molecular Medicine, Vol. 3. R. A. Meyers, editor. VCH Publishers, New York. 462–471.

Janshoff, A., and C. Steinem. 2001. Scanning force microscopy of artificial membranes. *Chem. Biochem.* 2:798–808.

Kamio, Y., and H. Nikaido. 1976. Outer membrane of *Salmonella typhimurium*: accessibility of phospholipid head groups to phospholipase C and cyanogen bromide activated dextran in the external medium. *Biochemistry.* 15:2561–2569.

Kastowsky, M., T. Gutberlet, and H. Bradaczek. 1993. Comparison of x-ray powder-diffraction data of various bacterial lipopolysaccharide structures with theoretical model conformations. *Eur. J. Biochem.* 217:771–779.

Kato, N., T. Sugiyama, N. Kido, M. Ohta, Y. Arakawa, S. Naito, H. Ito, and K. Sasaki. 1993. Crystallization and molecular structure of *Escherichia coli* Re and K-12 lipopolysaccharides. *In* Bacterial Endotoxin: Recognition and Effector Mechanisms. J. Levin, C. R. Alving, R.S. Munford, and P. L. Stutz, editors. Excerpta Medica, Amsterdam, The Netherlands. 49–60.

Kato, N., T. Sugiyama, S. Naito, Y. Arakawa, H. Ito, N. Kido, M. Ohta, and K. Sasaki. 2000. Molecular structure of bacterial endotoxin (*Escherichia coli* Re lipopolysaccharide): implications for formation of a novel heterogeneous lattice structure. *Mol. Microbiol.* 36:796–805.

Labischinski, H., G. Barnickel, H. Bradaczek, D. Nauman, E. T. Rietschel, and P. Giesbrecht. 1985. High state of order of isolated bacterial lipopolysaccharide and its possible contribution to the permeation barrier property of the outer membrane. *J. Bacteriol.* 162:9–20.

Luo, G., T. Liu, X. S. Zhao, Y. Huang, C. Huang, and W. Cao. 2001. Investigation of polymer-cushioned phospholipid bilayers in the solid phase by atomic force microscopy. *Langmuir.* 17:4074–4080.

Macias, E. A., F. R. Rana, J. Blazyk, and M. C. Modzrakowski. 1990. Bactericidal activity of magainin 2: use of lipopolysaccharide mutants. *Can. J. Microbiol.* 36:582–584.

Majewski, J., J. Y. Wong, C. K. Park, M. Seitz, J. N. Israelachvili, and G. S. Smith. 1998. Structural Studies of Polymer-Cushioned Lipid Bilayers. *Biophys. J.* 75:2363–2367.

McIntosh, T. J., A. D. Magid, and S. A. Simon. 1987. Steric repulsion between phosphatidylcholine bilayers. *Biochemistry.* 26:7325–7332.

McIntosh, T. J., A. D. Magid, and S. A. Simon. 1989. Cholesterol modifies the short-range repulsive interactions between phosphatidylcholine membranes. *Biochemistry.* 28:17–25.

Melikyan, G. B., N. S. Matinyan, and V. B. Arakelian. 1990. The influence of gangliosides on the hydrophilic pore edge line tension and monolayer fusion of lipid membranes. *Biochim. Biophys. Acta.* 1030:11–15.

Nikaido, H. 1994. Prevention of drug access to bacterial targets: permeability barriers and active efflux. *Science.* 264:382–388.

Nikaido, H., and M. Vaara. 1985. Molecular basis of bacterial outer membrane permeability. *Microbiol. Rev.* 49:1–32.

Oren, Z., and Y. Shai. 1997. Selective lysis of bacteria but not mammalian cells by diastereomers of melittin: structure-function study. *Biochemistry.* 36:1826–1835.

Pfau, A., W. Schrepp, and D. Horn. 1999. Detection of a single molecule adsorption structure of poly(ethylenimine) macromolecules by AFM. *Langmuir.* 15:3219–3225.

Raetz, C. R. H. 1993. Bacterial endotoxins: extraordinary lipids that activate eukaryotic signal transduction. *J. Bacteriol.* 175:5745–5753.

Rana, F. R., E. A. Macias, C. M. Sultany, M. C. Modzrakowski, and J. Blazyk. 1991. Interactions between magainin 2 and *Salmonella typhimurium* outer membranes: effect of lipopolysaccharide structure. *Biochemistry.* 30:5858–5866.

Reviakine, I., W. Bergsma-Schutter, and A. Brisson. 1998. Growth of protein 2-D crystals on supported planar lipid bilayers imaged in situ by AFM. *J. Struct. Biol.* 121:356–361.

Reviakine, I., and A. Brisson. 2000. Formation of supported phospholipid bilayers from unilamellar vesicles investigated by atomic force microscopy. *Langmuir.* 16:1806–1815.

Rietschel, E. T., T. Kirikae, F. U. Schade, U. Mamt, G. Schmidt, H. Loppnow, A. J. Ulmer, U. Zahringer, U. Seydel, F. DiPadova, and M. Schreier. 1994. Bacterial endotoxin: molecular relationships of structure to activity and function. *FASEB J.* 8:217–225.

Rinia, H. A., R. A. Kik, R. A. Demel, M. M. E. Snel, J. A. Killian, J. P. J. M. van der Eerden, and B. de Kruijff. 2000. Visualization of highly ordered striated domains induced by transmembrane peptides in supported phosphatidylcholine bilayers. *Biochemistry.* 39:5852–5858.

Rinia, H. A., M. M. E. Snel, J. P. J. M. van der Eerden, and B. de Kruijff. 2001. Visualizing detergent resistant domains in model membranes with atomic force microscopy. *FEBS Lett.* 501:92–96.

Rodriguez-Torres, A., M. C. Ramos-Sanchez, A. Ordufla-Domingo, F. J. Martin-Gil, and J. Martin-Gil. 1993. Differential scanning calorimetry investigating on LPS and free lipids A of the bacterial cell wall. *Res. Microbiol.* 144:729–740.

Samsonov, A. V., I. Mihalyov, and F. S. Cohen. 2001. Characterization of cholesterol-sphingomyelin domains and their dynamics in bilayer membranes. *Biophys. J.* 81:1486–1500.

Seitz, M., C. K. Park, J. Y. Wong, and J. N. Israelachvili. 2001. Long-range interaction forces between polymer-supported lipid bilayer membranes. *Langmuir.* 17:4616–4626.

Seitz, M., E. Ter-Ovanesyan, M. Hausch, C. K. Park, J. A. Zasadzinski, R. Zentel, and J. N. Israelachvili. 2000. Formation of tethered supported bilayers by vesicle fusion onto lipopolymer monolayers promoted by osmotic stress. *Langmuir.* 16:6067–6070.

Seitz, M., J. Y. Wong, C. K. Park, N. A. Alcantar, and J. N. Israelachvili. 1998. Formation of tethered supported bilayers via membrane-inserting reactive lipids. *Thin Sol. Films.* 327–329:767–771.

Senden, T. J., and W. A. Ducker. 1992. Surface roughness of plasma-treated mica. *Langmuir.* 8:733–735.

Seydel, U., and K. Brandenburg. 1990. Conformation of endotoxins and their relationship to biological activity. *In* Cellular and Molecular Aspects of Endotoxin Reactions. A. Nowotny, J. J. Spitzer, and E. J. Ziegler, editors. Excerpta Medica, Amsterdam, The Netherlands. 61–71.

Seydel, U., M. H. J. Koch, and K. Brandenburg. 1993b. Structural polymorphisms of rough mutant lipopolysaccharides Rd to Ra from *Salmonella minnesota*. *J. Struct. Biol.* 110:232–243.

Seydel, U., H. Labischinski, M. Kastowsky, and K. Brandenburg. 1993a. Phase behavior, supramolecular structure, and molecular conformation of lipopolysaccharide. *Immunobiology.* 187:191–211.

Shao, Z., J. Mou, D. M. Czajkowsky, J. Yang, and J.-Y. Yuan. 1996. Biological atomic force microscopy: what is achieved and what is needed. *Adv. Phys.* 45:1–86.

Snyder, S., D. Kim, and T. J. McIntosh. 1999. Lipopolysaccharide bilayer structure: effect of chemotype, core mutations, divalent cations, and temperature. *Biochemistry.* 38:10758–10767.

Snyder, S. and T. J. McIntosh. 2000. The lipopolysaccharide barrier: correlation of antibiotic susceptibility with antibiotic permeability and fluorescent probe binding kinetics. *Biochemistry.* 39:11777–11787.

Sohling, U., and A. J. Schouten. 1996. Investigation of the adsorption of dioleoyl-L-α-phosphatidic acid mono- and bilayers from vesicle solution onto polyethylenimine-covered substrates. *Langmuir.* 12: 3912–3919.

Takayama, K., D. H. Mitchell, Z. Z. Din, P. Mukerjee, C. Li, and D. L. Coleman. 1994. Monomeric Re lipopolysaccharide from *Escherichia coli* is more active than the aggregated form in the *Limulus* amebocyte lysate assay and in inducing Egr-1 mRNA in murine peritoneal macrophages. *J. Biol. Chem.* 269:2241–2244.

Tardieu, A., V. Luzzati, and F. C. Reman. 1973. Structure and polymorphism of the hydrocarbon chains of lipids: a study of lecithin-water phases. *J. Mol. Biol.* 75:711–733.

Veatch, S. L., and S. L. Keller. 2003. A closer look at the canonical ''raft mixture'' in model membrane studies. *Biophys. J.* 84:725–726.

Velegol, S. B., and B. E. Logan. 2002. Contributions of bacterial surface polymers, electrostatics, and cell elasticity to the shape of AFM force curves. *Langmuir.* 18:5256–5262.

Wagner, M. L., and L. K. Tamm. 2000. Tethered polymer-supported planar lipid bilayers for reconstitution of integral membrane proteins: silane-polyethyleneglycol-lipid as a cushion and covalent linker. *Biophys. J.* 79:1400–1414.

Wong, J. Y., J. Majewski, M. Seitz, C. K. Park, J. N. Israelachvili, and G. S. Smith. 1999a. Polymer-cushioned bilayers. I. A structural study of various preparation methods using neutron reflectometry. *Biophys. J.* 77:1445–1457.

Wong, J. Y., C. K. Park, M. Seitz, and J. N. Israelachvili. 1999b. Polymer-cushioned bilayers. II. An investigation of interaction forces and fusion using the surface forces apparatus. *Biophys. J.* 77:1458–1468.

Yao, X., W. S. Burke, S. Stewart, M. H. Jericho, D. Pink, R. Hunter, and T. J. Beverridge. 2002. Atomic force microscopy and theoretical considerations of surface properties and turgor pressures of bacteria. *Coll. Surf. B Biointerf.* 23:213–230.

Yuan, C., J. Furlong, P. Burgos, and L. J. Johnston. 2002. The size of lipid rafts: an atomic force microscopy study of ganglioside GM1 domains in sphingomyelin/DOPC/cholesterol membranes. *Biophys. J.* 82:2526–2535.

Zhang, L., C. A. Booth, and P. Stroeve. 2000. Phosphatidylserine/cholesterol bilayers supported on a polycation/alkylthiol layer pair. *J. Colloid Interface Sci.* 228:82–89.

Zhang, L., R. Vido, A. J. Waring, R. I. Lehrer, M. L. Longo, and P. Stroeve. 2002. Electrochemical and surface properties of solid-supported, mobile phospholipid bilayers on a polyion/alkylthiol layer pair used for detection of antimicrobial peptide insertion. *Langmuir*. 18:1318–1331.

Zimmermann, W., and A. Rosselet. 1977. Function of the outer membrane of *Escherichia coli* as a permeability barrier to beta-lactam antibiotics. *Antimicrob. Agents Chemother*. 12:368–372.